Picosecond Time-resolved Absorption and Fluorescence Dynamics in the Artificial Bacteriorhodopsin Pigment BR6.11

T. L. Brack,* J. K. Delaney,* G. H. Atkinson,*‡ A. Albeck,§¶ M. Sheves,‡§ and M. Ottolenghi,‡‖

*Department of Chemistry and Optical Science Center, University of Arizona, Tucson, Arizona 85721 USA; §Department of Organic Chemistry, Weizmann Institute, Rehovot, Israel; ‖Department of Physical Chemistry, Hebrew University, Jerusalem

ABSTRACT The picosecond molecular dynamics in an artificial bacteriorhodopsin (BR) pigment containing a structurally modified all-*trans* retinal chromophore with a six-membered ring bridging the C_{11}=C_{12}—C_{13} positions (BR6.11) are measured by picosecond transient absorption and picosecond time-resolved fluorescence spectroscopy. Time-dependent intensity and spectral changes in absorption in the 570–650-nm region are monitored for delays as long as 5 ns after the 7-ps, 573-nm excitation of BR6.11. Two intermediates, J6.11 and K6.11/1, both with enhanced absorption to the red (>600 nm) of the BR6.11 spectrum are observed within ~50 ps. The J6.11 intermediate decays with a time constant of 12 ± 3 ps to form K6.11/1. The K6.11/1 intermediate decays with an ~100-ps time constant to form a third intermediate, K6.11/2, which is observed through diminished 650-nm absorption (relative to that of K6.11/1). No other transient absorption changes are found during the remainder of the initial 5-ns period of the BR6.11 photoreaction.

Fluorescence in the 650–900-nm region is observed from BR6.11, K6.11/1, and K6.11/2, but no emission assignable to J6.11 is found. The BR6.11 fluorescence spectrum has a ~725-nm maximum which is blue-shifted by ~15 nm relative to that of native BR-570 and is 4.2 ± 1.5 times larger in intensity (same sample optical density). No differences in the profile of the fluorescence spectra of BR6.11 and the intermediates K6.11/1 and K6.11/2 are observed. Following ground-state depletion of the BR6.11 population, the time-resolved fluorescence intensity monitored at 725 nm increases with two time constants, 12 ± 3 and ~100 ps, both of which correlate well with changes in the picosecond transient absorption data.

The resonance Raman spectrum of ground-state BR6.11, measured with low-energy, 560-nm excitation, is significantly different from the spectrum of native BR-570, thus confirming that the picosecond transient absorption and picosecond time-resolved fluorescence data are assignable to BR6.11 and its photoreaction alone and not to BR-570 reformed during the reconstitution process (<5% of the BR6.11 sample could be attributed to native BR-570).

The J6.11 and K6.11 absorption and fluorescence data presented here are generally analogous to those measured for native J-625 and K-590, respectively, and therefore, the primary events in the BR6.11 photoreaction can be correlated with those in the native BR photocycle. The BR6.11 photoreaction, however, exhibits important differences including slower formation rates for J and K intermediates as well as the presence of a second K intermediate. These results demonstrate that the restricted motion in the C_{11}=C_{12}—C_{13} region of retinal found in BR6.11 does not greatly change the overall photoreaction mechanism, but does alter the rates at which processes occur.

INTRODUCTION

The replacement of the all-*trans* retinal chromophore found in native bacteriorhodopsin (BR), *Halobacterium halobium*, with structurally modified retinals to form artificial BR pigments has proven to be exceptionally valuable in elucidating many aspects of the native BR photocycle (1). The reconstitution techniques that underlie the preparation of artificial BR pigments can be utilized with a wide range of structurally altered retinal chromophores and therefore, many different artificial BR pigments are available (1). Time-resolved absorption and fluorescence measurements provide opportunities to identify the relationships between the molecular structure of the retinal chromophore, the photoreaction dynamics, and the overall biochemical functionality (i.e., proton pumping) found in each artificial pigment. Both the molecular properties of the chromophore (e.g., electronic structure, the rotational degrees of freedom around C—C and C=C bonds, and the presence of steric hindrance caused by bulky substitutes) and the interactions between retinal and its protein environment can be systematically examined. The photoreaction of each artificial BR pigment is itself independently important with respect to applications such as optical data storage and processing (2, 3).

Artificial BR pigments with retinals containing rings located in the polyene backbone structure are of special interest biophysically since, in principle, each ring can be used to selectively restrict and/or block molecular motion at specific C—C and C=C bonds. Nakanishi and coworkers (4) were the first to recognize the importance of introducing ring structures into the polyene chain. The retinal structure around the C—C and C=C bonds has long been recognized as one important factor in the BR photocycle (1, 4–7). Specifically, isomerization around the retinal C=C bonds has been considered a fundamental step in the primary (femto/picosecond) energy storage events in retinal-containing proteins (e.g., *trans* to *cis* isomerization at the C_{13}=C_{14} bond (1, 4–7) in BR and *cis* to *trans* isomerization at the C_{11}=C_{12}

Received for publication 19 January 1993 and in final form 23 April 1993.

‡Authors to whom correspondence should be addressed.

¶Present address: Department of Chemistry, Bar Ilan University, Ramat Gan, Israel.

0006-3495/93/08/964/09 $2.00

bond in rhodopsin (8)). Some artificial BR pigments containing retinals with ring structures prevent isomerization at specific C=C bonds and, therefore, provide opportunities to correlate C=C isomerization with particular parts of the BR photocycle. Orientation around C—C bonds is no less important. For example, it has been shown that the conformation between the ionone ring and the polyene chain of the retinal chromophore in BR is planar s—*trans* in contrast to the s-*cis*, twisted conformation found in solution (9). Other twisting around C—C bonds of the retinal in BR also has been recently demonstrated (10). Thus, the selective introduction of ring structures into the polyene backbone also can alter the degree of nonplanarity (i.e., twisting) in the retinal chromophore, thereby affecting not only the degrees of freedom in retinal itself, but also the corresponding chromophore-protein interactions. The relationships, if any, between the degree of retinal planarity and the photocycle mechanism remain to be established.

Only a few studies of the femto/picosecond dynamics in artificial BR pigments have been reported (11–14) and, as a consequence, it remains unclear whether femto/picosecond intermediates analogous to J-625 and K-590 in native BR are formed when all-*trans* retinal is structurally altered. It has been shown that the artificial BR pigment containing 13-demethyl (13-dm) retinal does produce J13-dm and K13-dm (12–14). Such studies of artificial BR pigments encompass a variety of experimental challenges which must be successfully addressed. These include the preparation of the relatively large quantities of artificial BR pigments needed to perform time-resolved spectroscopic measurements, the effective, high yield reconstitution of the structurally modified retinal with the apoprotein opsin, and the photochemical stability of the resultant artificial BR pigments under mechanical pumping required to form liquid jet samples for laser excitation.

In this paper, the picosecond dynamics following the 7-ps optical excitation of an artificial BR pigment containing a structurally modified all-*trans* retinal chromophore (*E*-11,20-ethanoretinal) with a six-membered ring bridging the C_{11}=C_{12}—C_{13} positions (Fig. 1) are measured by time-resolved absorption and fluorescence spectroscopy. This artificial BR pigment is denoted as BR6.11 indicating that it contains a retinal chromophore with a six-membered ring starting at C_{11}. Picosecond transient absorption and picosecond time-resolved fluorescence measurements record, respectively, the time-dependent changes in the absorption and fluorescence from BR6.11 samples. Fluorescence spectra, measured from ground-state samples and time-resolved intermediates, together with the vibrational resonance Raman spectrum of ground-state BR6.11, also are presented to further characterize the BR6.11 sample and its photoreaction.

Previous studies have shown that BR6.11 (i) has a photoreaction containing both a K intermediate (observed on the >50-ns time scale) (15) and an M intermediate (absorbing near 420 nm) (15) and (ii) pumps protons across the BR membrane (15). In the work presented here, it is shown that both J- and K-like intermediates (J6.11 and K6.11/1) are observed within 50 ps of 573-nm excitation of BR6.11. The J6.11 intermediate has an absorption spectrum which is red-shifted (maximum near 610 nm) relative to both BR6.11 and K6.11/1. The K6.11/1 intermediate has enhanced absorption to the red of that from BR6.11, although its absorption maximum is not clearly determined in this study. The J6.11 decays to K6.11/1 with a 12 ± 3-ps time constant. A third intermediate, K6.11/2, is observed to have diminished absorption near 650 nm and appears with a time constant of ~100 ps as K6.11/1 decays. Fluorescence from BR6.11 and the K6.11/1 and K6.11/2 intermediates are found, but no emission from the J6.11 intermediate is observed. The unique vibrational structure of ground-state BR6.11 is established through its resonance Raman spectrum which also serves to confirm that the artificial BR pigment sample contains almost exclusively BR6.11. The results presented here demonstrate that neither isomerization nor rotations around the C_{11}=C_{12} nor C_{12}—C_{13} bonds, respectively, are prerequisites for the formation of J6.11, K6.11/1, or K-6.11/2.

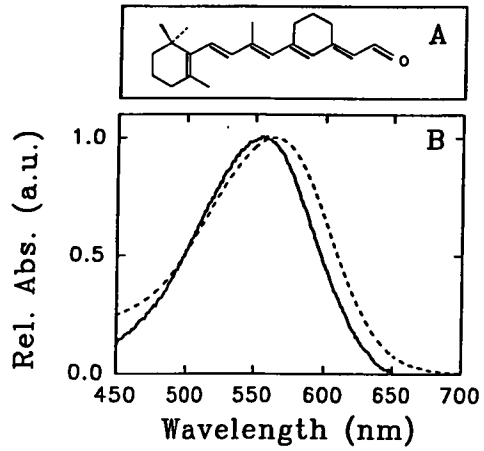

FIGURE 1 (*A*) Chemical structure of retinal 6.11 (*E*-11,20-ethanoretinal). (*B*) The normalized absorption spectra of BR6.11 (*solid line*) and native BR-570 (*dashed line*) uncorrected for scattering from the purple membranes.

EXPERIMENTAL PROCEDURE

The retinal analog *E*-11,20-ethanoretinal (retinal 6.11) is synthesized as previously described (15). The apoprotein, bacterio-opsin, is obtained by optically bleaching BR, grown from the S9 strain of *Halobacterium halobium*, in the presence of hydroxyl amine in order to bind the freed retinal in an oxime-retinal complex. The bleached opsin sample, including the oxime-retinal complex, is mixed with a sample of the retinal 6.11 chromophore dissolved in ethanol in order to obtain the reconstituted artificial BR6.11 pigment (total volume of 20 ml). The reconstitution of BR6.11, requiring ~1 day to complete at ~300K, is monitored via the increasing BR6.11 absorption at 556 nm and the corresponding decrease of the retinal 6.11 absorption at 380 nm. The optical density of the resulting BR6.11 sample is typically between 1.5 and 2.5 (at λ_{max}). The pH of the resultant artificial BR6.11 sample without buffers is ~6.5. The flowing BR6.11 sample is light-adapted by exposure to the emission of an incandescent lamp (60 watts) for at least 10 min prior to each experiment. It has been shown that following light adaptation, the BR6.11 mixture contains a 9:1 ratio of *trans* to *cis* retinal isomers in the binding site (15).

The instrumentation and procedures utilized to obtain picosecond transient absorption and picosecond time-resolved fluorescence spectroscopy

have been discussed in detail previously (16, 17) and therefore, only a brief description is given here. The 532-nm, second-harmonic output from a Nd:YAG (Quantronix) laser synchronously pumps two cavity-dumped dye lasers (Coherent 702) each operating at a 1-MHz repetition rate. The wavelengths of the 7-ps (FWHM) pulses from the dye lasers can be tuned continuously within the 560–620-nm (Rhodamine 6G) and 620–665-nm (Rhodamine 640) ranges. The dye laser pulsewidths, measured by autocorrelation, are ~7 ps (FWHM). The cross correlation time (CCT), defined by the temporal overlap between the two dye laser pulses, is ~12 ps (FWHM) and is used to determine that the timing jitter during these pump-probe measurements is ± 3.4 ps (18). Generally, the dye laser used to initiate the photoreaction is operated at ~10 mW, while the probe laser power is selected to be 2–6 mW. The time delays between the pump and probe laser pulses are obtained over the 5-ns time interval examined here by changing the optical delay line located in the path of the probe laser pulses. The pump and probe laser beams are colinearly recombined before they are both directed to the BR6.11 sample.

The BR6.11 sample is examined as a flowing liquid jet (~350 μm diameter) moving at ~20 m/s and created by mechanical pumping through a cylindrical, glass nozzle. Typically, 15 ml of BR6.11 at OD 2.5 is used. The temperature of the sample is maintained at 10°C to minimize thermal degradation of BR6.11. The pump and probe laser beams are focused to an ~20-μm diameter spot within the flowing liquid jet. The spot size together with the 1-MHz repetition rates of the lasers and the velocity of the liquid ensure that the sample volume exposed to one pair of pump-probe pulses is removed completely from the optical path prior to the arrival of the next pair of laser pulses.

The picosecond transient absorption (PTA) signals are measured by monitoring the intensity of the probe laser beam after it passes through the sample jet. The probe pulses are spectrally separated from the pump beam by reflection from a 1200 line/mm grating before the pulse energy is measured by a photodiode (EG&G HUV-2000B). The photodiode signal is processed by a lock-in amplifier synchronized with the frequency of a mechanical chopper placed in the optical path of the pump laser beam.

Picosecond time-resolved fluorescence (PTRF) measurements monitor the total photoreaction fluorescence initiated by a selectively delayed probe laser (560–665 nm) pulse. The PTRF signal measured with a given time-delayed probe pulse, therefore, contains contributions from all fluorescing species present in the photoreaction mixture (stable and transient intermediates). The fluorescence is collected at right angles to the plane formed by the sample jet and the two laser beams and focused onto the entrance slit (1 mm) of a 1-m, single monochromator (model 1704; Spex) having a 1200 line/mm grating. The wavelength dispersed fluorescence is imaged onto the face of a cooled PMT (model R-943/02; Hamamatsu Corp.). The PMT signal is processed by a lock-in amplifier that is referenced to the frequency of a mechanical chopper placed in the probe laser beam in order to ensure that only fluorescence induced by the probe pulses are measured. The overall spectral bandpass of the detection system is 1.2 nm centered at 725 nm (the maximum of BR6.11 fluorescence, vide infra). To eliminate stray light and reduce Raleigh scattering, glass cut-off filters (Corning 2-26, 2-63, and 2-59 and Melles Griot 03FCG109 and 03FCG111) are placed between the sample and the entrance slit of the monochromator.

The resonance Raman (RR) spectrum from ground-state BR6.11 is recorded with picosecond pulsed excitation from only one of the dye lasers. The RR scattering is collected and focused onto the entrance slit of a triple monochromator (Triplemate; Spex) equipped with two 600 line/mm gratings (double monochromator operated in subtractive dispersion) and a 600 line/mm concave grating (operated as a dispersive monochromator). The dispersed RR scattering is measured by an intensified, multichannel detector (model 1420HQ, PARC Reticon) which can view ~1000 cm^{-1} simultaneously.

RESULTS

PTA in BR6.11

The PTA data measured with probe wavelengths of 568, 590, 610, 620, and 650 nm and over the initial 110 ps of the photocycle contain absorption changes (ΔA) which can be assigned to two intermediates, namely J6.11 and K6.11/1. Three picosecond transient absorption traces representative of these data throughout the 568–650-nm region are presented in Fig. 2. From these data alone, it is evident that the J6.11 and K6.11/1 intermediates each have enhanced absorption to the red of that from BR6.11. A rapid, <5-ps (i.e., within the CCT) change in absorption is observed in the 620–650-nm PTA data (e.g., Figs. 2, *B* and *C*). These ΔA changes are attributed to J6.11. No corresponding <5-ps ΔA increase is found in the 568-nm PTA data, but rather a much slower (12 ± 3 ps) increase appears following the initial ΔA decrease within the CCT (Fig. 2 *A*). This 12 ± 3-ps ΔA increase reflects the formation of K6.11/1. Indeed, the presence of K6.11/1 can be observed in the PTA data throughout

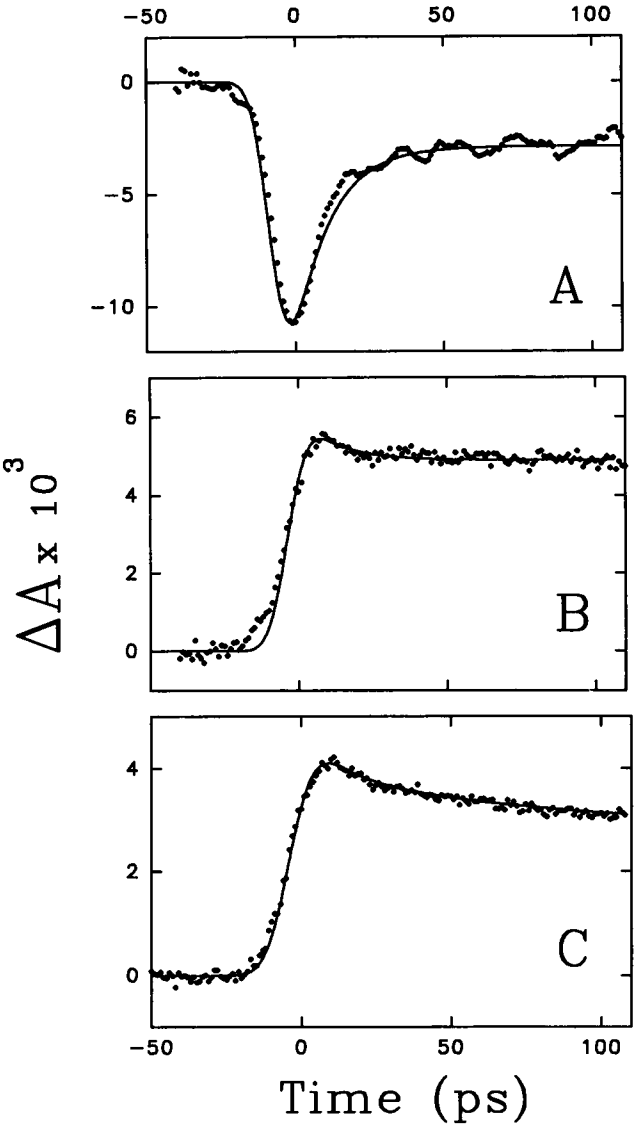

FIGURE 2 PTA data (*filled circles*) from BR6.11 following 7-ps, 573-nm excitation during the initial 110 ps of the BR6.11 photoreaction. Probe wavelengths of (*A*) 568, (*B*) 620, and (*C*) 650 nm are used to represent PTA data recorded throughout the 568–650-nm region. The solid lines represent fits to specific PTA data based on the convolution of the cross correlation time defined by the pump and probe laser pulses with a kinetic model: BR6.11 + $h\nu$ → BR*6.11 → J6.11 → K6.11/1 → K6.11/2. See text for details.

the 568–650-nm region, since this intermediate maintains some absorbance at all of these probe wavelengths. The enhanced absorption in the 600–650-nm region relative to BR6.11 is manifested in the increasingly large ΔA values measured at delays times greater than 50 ps (Figs. 2, *B* and *C*).

PTA data recorded at 650 nm reveal that a second K-like intermediate, denoted K6.11/2, is formed over the 50–500-ps interval. Between 50 and 500 ps, the 650-nm PTA signal decreases with an ~100-ps time constant (Fig. 3) before becoming constant over the 500-ps to 5-ns interval (data not shown). The ~100-ps decrease indicates that K6.11/1 transforms into K6.11/2 which has a smaller absorption coefficient at 650-nm than that of K6.11/1. No ΔA changes are observed within the 50–500-ps interval in PTA data recorded with probe wavelengths in the 568–630-nm region. The absorption spectra of K6.11/1 and K6.11/2, therefore, must be similar except at wavelengths near or to the red of 650 nm.

The general kinetics describing the early stages of the BR6.11 photoreaction can be obtained from these PTA data. The time constants (τ) of the J6.11 → K6.11/1 and K6.11/1 → K6.11/2 transformations are permitted to vary in the kinetic analysis in order to obtain the best fits to the PTA data. Examples of the resultant fits are shown in Figs. 2 and 3. The kinetics describing the ground-state populations of J6.11, K6.11/1, and K6.11/2 as observed from PTA after 7-ps, 573-nm excitation can be summarized as: (i) <5-ps (i.e., within CCT) formation of J6.11 followed by decay to K6.11 with a τ of 12 ± 3 ps, (ii) decay of K6.11/1 to K6.11/2 with a τ of ~100 ps, and (iii) K6.11/2 is present at least 5 ns after BR6.11 is excited with no apparent decay (data not shown).

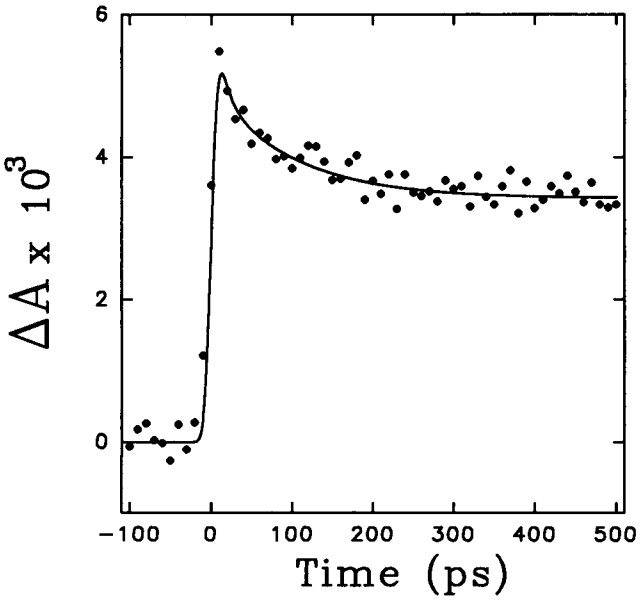

FIGURE 3 PTA data (filled circles#) at 650 nm from BR6.11 following 7-ps, 573-nm excitation over the initial 500-ps interval of the BR6.11 photoreaction. A decreasing ΔA is observed in the 50–500-ps interval that is not found at probe wavelengths <620 nm. The solid line represents a fit derived from the same kinetic model described for Fig. 2. A separate decay process (~100-ps time constant) is observed between 50–500 ps revealing the presence of K6.11/2. See text for details.

In general, the PTA signals from J6.11 and K6.11/1 (Fig. 2) resemble those measured in native BR over the same wavelength region that revealed the presence of the J-625 and K-590 intermediates (17, 19, 20). The transient absorption spectra of the J6.11 and K6.11/1 intermediates, therefore, are anticipated to be similar to that of J-625 and K-590, respectively. The absorption spectra of J6.11 and K6.11/1 are derived from an analysis of all the 568–650-nm PTA results using the kinetic model:

$$\text{BR6.11} + h\nu \rightarrow \text{BR6.11}^* \ (<5 \text{ ps}) \rightarrow \text{J6.11} \ (\tau = 12 \pm 3 \text{ ps}) \rightarrow \text{K6.11/1} \ (\tau \approx 100 \text{ ps}) \rightarrow \text{K6.11/2}, \quad (1)$$

in which the quantum efficiency for the formation of J6.11 is taken to be 0.6.

The resultant absorption spectra assignable to J6.11 and K6.11/1 are presented in Fig. 4. Two isobestic points are observed in the PTA data recorded in the 568–650-nm spectral region. The first, at 610 nm, appears during the initial 50-ps period of the BR6.11 photoreaction and, therefore, is associated with the J6.11 → K6.11/1 transformation. The second, at 590 nm, is observed at delay times longer than 50 ps and is associated with BR6.11 and K6.11 (i.e., K6.11/1 and K6.11/2 have the same absorbance at 590 nm). The observation in the PTA measurements of two distinct isobestic points at different times supports the conclusion that three distinct species (J6.11, K6.11/1, and K6.11/2) connected by two sequential reactions are present.

Fluorescence spectra from BR6.11 and its photoproducts

Fluorescence from BR6.11 is recorded by using picosecond laser excitation with sufficiently low pulse energies (~2 nJ/

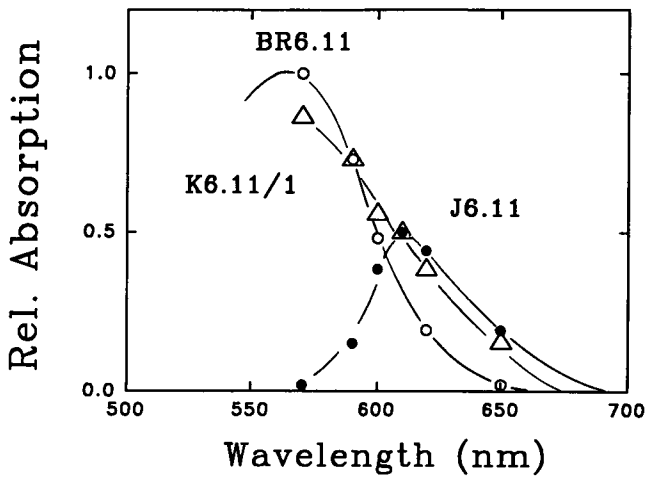

FIGURE 4 Relative absorption spectra of BR6.11 (*unfilled circles*) and the J6.11 (*filled circles*) and K6.11/1 (*unfilled triangles*) intermediates. Spectra are derived from kinetic fits to PTA (e.g., Fig. 2) based on the photoreaction: BR6.11 + $h\nu$ → BR*6.11 → J6.11 → K6.11/1 → K6.11/2 (assuming a quantum yield for BR*6.11 → J6.11 of 0.6). Two isobestic points are measured at different time delays: 590 nm (BR6.11 → K6.11/1) at > 50-ps delays and 610 nm (J6.11 → K6.11/1) at ~50-ps delay.

pulse) to ensure that no significant photochemistry occurs and, therefore, that only fluorescence from the excited electronic state of BR6.11 (BR*6.11) is measured. The BR*6.11 fluorescence spectrum, obtained with 599-nm excitation, extends from ~600 to 900 nm and has a broad maximum centered near 725 nm (Fig. 5). The spectral shape of fluorescence from BR*6.11 is similar to that from native BR*-570, although the two can be readily distinguished since the BR*6.11 fluorescence maximum is shifted by ~15 nm to the blue (Fig. 5). It also is important to note that the total fluorescence intensity from BR*6.11 is 4.2 ± 1.5 times larger than that observed from native BR* (16, 21) (equal OD at the excitation wavelength). The intensity maxima of the two spectra have been scaled in Fig. 5 to facilitate a comparison of the spectral profiles.

The time resolved fluorescence spectra of the intermediates recorded at 160 and 300 ps after initiation of the BR6.11 photoreaction show no significant change in either position or intensity (within ~20%) from that observed from BR*6.11 (Fig. 5).

PTRF from the BR6.11 photoreaction

Time-dependent changes in the fluorescence intensity during the BR6.11 photoreaction are measured near the 725-nm spectral maximum (Fig. 5) as the probe laser pulse used to initiate fluorescence from the sample is delayed relative to the 7-ps, 573-nm excitation of BR6.11. These PTRF data monitor changes in both the ground-state populations and the relative efficiencies with which each of the populated excited electronic states emit (e.g., K*6.11/1 versus BR*6.11). Since the ground-state populations are independently monitored via picosecond transient absorption, a quantitative comparison of PTRF and picosecond transient absorption data can be utilized to determine the fluorescence properties of excited electronic states during the photoreaction. The PTRF signal recorded from BR6.11 over the initial 500-ps period of the photoreaction is presented in Fig. 6.

The depletion of the ground-state BR6.11 population, observed within the CCT, is followed by two sequential increases in fluorescence intensity characterized by two time constants, 12 ± 3 ps followed by ~100 ps. The kinetic fit from which these time constants are derived is shown in Fig. 6. The 12 ± 3 ps time constant correlates well with the picosecond transient absorption data (Fig. 2) and is assigned to the J6.11 → K6.11/1 transformation. The ~100-ps time constant corresponds to the picosecond transient absorption change associated with K6.11/1 → K6.11/2 (Fig. 3). The PTRF data, however, has no fast (<5 ps, CCT) component such as that observed in the picosecond transient absorption results and assigned to the formation of J6.11. The absence of such a fast component in the PTRF signal suggests that, like J-625 in the native BR photocycle, J6.11 does not emit in the 650–900-nm region.

RR scattering from BR6.11

The vibrational RR spectrum of BR6.11 recorded with low-energy (1.8 mW), 560-nm excitation is presented in Fig. 7. No evidence of photochemical changes is evident following such low-energy excitation and, therefore, this RR spectrum is assigned to ground-state BR6.11 alone. The RR spectrum from native BR-570 also is shown in Fig. 7 as a dashed trace in order to emphasize the differences in the vibrational band positions and relative intensities (vide infra). The band maxima positions of the significant features together with estimates of their relative intensities are listed in Table 1 for both BR6.11 and native BR-570.

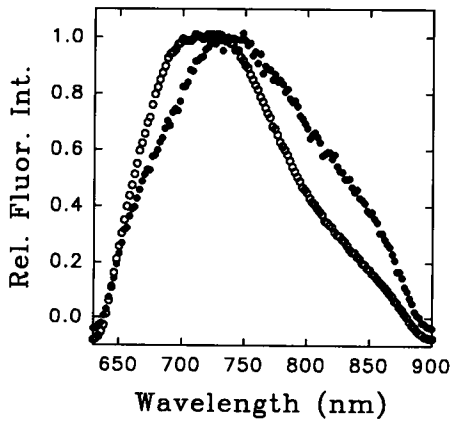

FIGURE 5 Fluorescence spectra of BR6.11 (*unfilled circles*) compared to that of native BR-570 (*filled circles*). The fluorescence intensity from BR6.11 is 4.2 ± 0.5 times larger than that from native BR-570 (samples have the same optical density at the 599-nm exulative wavelength). The intensity maxima of the two spectra are normalized to facilitate comparison of spectral band shapes and maxima positions. These data are uncorrected for the spectral response of the detection system.

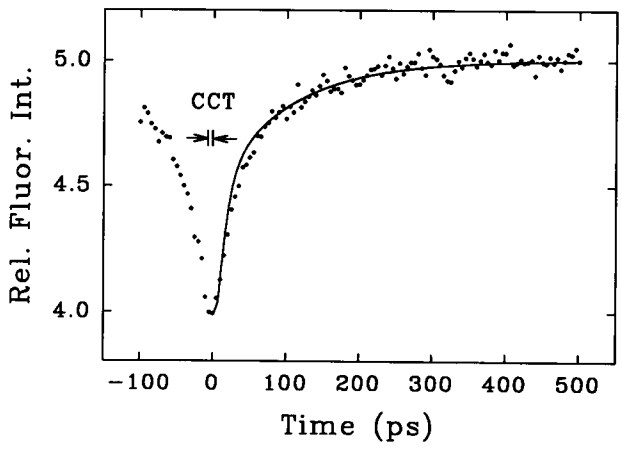

FIGURE 6 PTRF from BR6.11 (*filled circles*) following 7-ps, 573-nm excitation. The fluorescence is initiated at variable time delays after 573-nm excitation by 630-nm probe laser pulses. The fit shown for the 0–500-ps interval (*solid line*) is based on the kinetic model describing the BR6.11 photoreaction (see text). Two time constants (~12 ± 3 ps and ~100 ps) are observed in the PTRF signal and are assigned to the formation of K6.11/1 and K6.11/2, respectively. A schematic representation of the cross correlation time (HWFM) is presented as CCT.

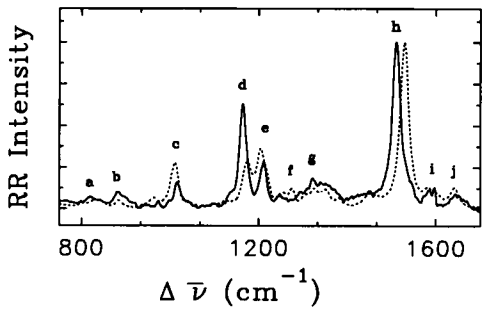

FIGURE 7 RR spectra of ground-state native BR-570 (*dashed line*) and BR6.11 (*solid line*) using low-energy, 560-nm excitation. The C=C stretching bands are normalized in the two RR spectra in order to reveal the significant differences in both band positions and relative intensities. For example, the 1164 cm^{-1} band in the fingerprint (C—C stretching) region is readily distinguished in BR6.11. The band maxima positions and relative intensities for BR6.11 and native BR are listed in Table 1.

TABLE 1 Band maxima positions and relative intensities of resonance Raman features for BR6.11 and native BR-570. Excitation at 560 nm for both

	BR6.11		BR-570	
Band*	Maxima position	Rel. int.‡	Maxima position	Rel. int.§
	cm^{-1}		cm^{-1}	
a	819	0.08	829	0.05
b	894	0.11	880	0.05
c	1016	0.17	1007	0.27
d	1164	0.63	1171	0.28
e	1210	0.30	1202	0.36
f	1247	0.11	1272	0.12
g	1323	0.20	1322	0.12
h	1511	1.00	1526	1.00
i	1586	0.14	1579	0.14
j	1640	0.11	1639	0.13

* Bands labelled by letters in Fig. 8 refer to BR6.11 (solid line) and native BR-570 features appearing near one another (dashed line).
‡ Normalized to the intensity of the 1511 cm^{-1} band.
§ Normalized to the intensity of the 1526 cm^{-1} band.

DISCUSSION

Isomerization from a *trans* to *cis* configuration at the C_{13}=C_{14} bond is widely viewed as the primary *structural* event in retinal required to initiate the native BR photocycle (1, 4–7). The reaction dynamics in artificial BR pigments have been examined with a variety of experimental techniques in order to determine which, if any, structural changes in retinal occur when (i) J and K intermediates are formed and (ii) a BR photoreaction produces an M-like intermediate (i.e., deprotonated Schiff base) and subsequently, initiates proton pumping. The BR6.11 data described here provide an opportunity to determine whether specific structural changes in the C_{11}=C_{12}—C_{13} region of retinal are required either for the formation of J and K intermediates or the appearance of the M intermediate and/or for proton pumping to occur.

RR

The 560-nm RR spectra presented in Fig. 7 confirm the expectation that the retinal vibrational degrees of freedom in BR6.11 and native BR-570 are significantly different. The structural differences in the retinal chromophore of BR6.11 from which resonantly enhanced Raman scattering is generated are clearly reflected throughout the 800–1700-cm^{-1} region. Special attention should be given to the C—C stretching (1100–1250 cm^{-1}) and C=C stretching (1450–1600 cm^{-1}) regions (Fig. 7 and Table 1). Essentially all the major BR6.11 RR bands in both spectral regions appear at new frequency displacements relative to those found in the RR spectrum of native BR-570. In addition, the relative intensities of several BR6.11 RR bands are different with the increased intensity of the 1164 cm^{-1} C—C stretching band being the most notable. The intensities of the C=C stretching bands have been normalized to facilitate comparisons of relative band intensities in the two spectra.

The 560-nm RR spectrum of BR6.11 is used here primarily to demonstrate that the reconstituted artificial BR pigment sample is comprised of BR6.11 and does not contain significant amounts of native BR-570 obtained by the reincorporation of all-*trans* retinal freed from the retinal-oxime complex during reconstitution. Since 560-nm excitation is in resonance with both the BR6.11 and BR-570 absorption spectra (Fig. 1), resonantly enhanced Raman scattering will contain contributions from both if either is present in significant amounts. Quantitative comparisons of band intensities relative to the measured signal to noise in RR spectra from native BR-570 and BR6.11 demonstrate that <5% (if any) of the artificial BR pigment sample can be attributed to reconstituted all-*trans*, native BR-570. Since the PTA and PTRF measurements are made on the same BR samples, the absorbing chromophores monitored in both also must be BR6.11 and the intermediates formed during its photoreaction. There is no evidence that BR-570 containing all-*trans* retinal formed during the reconstitution process makes any significant contribution to either the PTA or PTRF data.

PTA

The formation of J6.11 observed by PTA is analogous to that of J-625 in the native BR photocycle, i.e, the red-shift in sample absorbance together with its <5-ps appearance time follows closely the spectral and kinetic properties of J-625. In analogy with the native BR photocycle, the formation of J6.11 is the first BR6.11 photoreaction event observed by PTA in this time regime. The differences between the PTA data from J6.11 and J-625 involve the quantitative kinetics observed. The 12 ± 3-ps time constant of the decay of J6.11 to K6.11/1 is significantly longer than the 3.5-ps time constant measured for the transformation of native J-625 into K-590 (17, 20).

The slower reaction rates may reflect differences in the retinal-protein transformation(s) by which the K intermediates are formed from their respective J precursors. The different J → K rates also may be associated with alterations in the intrinsic retinal structure and/or alterations in the retinal-protein interactions caused by the introduction of the six-membered ring found in BR6.11. Both interpretations emphasize the importance of the retinal structure in determining

the molecular mechanism, and thereby the observed photoreaction rates. The data presented here demonstrate that the differences in retinal structures between BR6.11 and native BR-570 are sufficient to alter the reaction rates, but not to change the primary events in the photoreaction mechanism involving a J intermediate.

The absorption properties of K6.11/1 also are similar to those of native K-590, i.e., both have enhanced absorption to the red of the stable BR pigments (BR6.11 and BR-570, respectively) and blue-shifted relative to the initial photoreaction intermediate (J6.11 and J-625, respectively). It should be noted, however, that the K6.11/1 absorption is not shifted much relative to that from BR6.11 (unlike the native BR-570/K-590 case) and therefore, a distinct absorption maximum for K6.11/1 is not observed (Fig. 4).

PTA data monitoring the K intermediates do differ over the 50–500-ps interval. The reduced absorption from K6.11/2 at 650 nm over this time period (Fig. 3) reveals an ~100-ps transformation in the BR6.11 photoreaction not seen via absorption in the native BR photocycle. This same ~100-ps transformation, however, is observed in PTRF signals from K6.11/1 (Fig. 6). No additional change in the BR6.11 absorption at 650 nm is found over the 500- to 5-ns period which is analogous to the PTA kinetic found in the native BR photocycle.

With regard to this last point, it is important to note that PTA data (23) have recently been obtained which show that the KL intermediate proposed previously to appear in during the initial 10-ns interval of the native BR photocycle (19, 22) is not observed following low-power, 7-ps pulsed excitation. Rather, a change in the PTRF signal from native K-590 is found (24); specifically, the total fluorescence intensity decreases by ~80% with a time constant of 5.5 ns before reaching a constant value for delays of 10–100 ns (23).

The formation of K6.11/2 may reflect changes in either retinal itself or in the retinal-protein interactions during the lifetime of K6.11/1. This PTA observation during the 50–500-ps period of the BR6.11 photoreaction may be related to the 1–80-ns fluorescence measurement made recently in native BR photocycle (23). If the underlying molecular phenomena are related, then it suggests that different retinal-protein interactions can affect the ground-state absorption (PTA) and/or excited electronic state relaxation properties (PTRF). Within this context, it appears that K6.11/1 is a perturbed ground electronic state intermediate (e.g., vibrationally excited or structurally distorted) intermediate which relaxes with an ~100-ps time constant. Vibrational excitation seems unlikely given the observation that vibrational relaxation in BR occurs significantly faster than 10 ps (17, 24, 25). Structural distortion, in the retinal itself, in the protein environment or in both, is a more general explanation since it could alter both ground (absorption) and excited (fluorescence) electronic state properties. The ~100-ps K6.11/1 → K6.11/2 relaxation process, therefore, would represent structural changes in the retinal chromophore specific to a retinal containing a six-membered ring which is not present in the all-*trans* retinal chromophore. It is useful to note that more than one K form also has been reported from low temperature studies of native BR and are attributed to different conformations of BR-570 (26). The 5.5-ns relaxation process observed via fluorescence in the native BR photocycle (23) may not necessarily have an analogy in the BR6.11 photoreaction.

Fluorescence spectra and PTRF

Comparisons of the fluorescence spectra and time-dependent fluorescence intensities (PTRF data) from BR*6.11 and BR* suggest that the ground- and excited-state potential surfaces in the two pigments are similar, but that the relaxation dynamics in the two fluorescing excited electronic states are different. The spectral regions covered by fluorescence are the essentially same (650–900 nm, Fig. 5). The respective spectral shapes and the intensity maxima, however, differ. The BR*6.11 fluorescence profile has more intensity in the 650–725-nm region and less intensity in the 725–900-nm region (Fig. 5). The resultant intensity maximum for BR*6.11 is broad with a center near 725 nm (~15 nm to the blue of the BR*-570 intensity maximum at 740 nm (16)). The increased (i.e., 4.2 ± 1.5 times) fluorescence intensity from BR*6.11 indicates that relaxation via radiative channels is more effective than in native BR*-570. The competition between the nonradiative and radiative decay processes in both, however, remains strongly in favor of nonradiative decay, since the quantum yields of fluorescence are extremely small (~1–5 × 10^{-4} (21)). The increased fluorescence may also arise from differences in the retinal-protein interactions associated with the structurally modified retinal in BR6.11, vide supra. Substantial changes in the fluorescence intensity have been observed during the photoreactions of both artificial (14) and native (16, 23, 27) BR pigments which can be attributed to alterations in retinal-protein interactions. The larger amount of fluorescence also may be associated with a correspondingly longer excited electronic state lifetime for BR*6.11 relative to that for BR*-570 (~500 fs (20)). Such a 2–3-ps BR*6.11 lifetime is not directly observable in the picosecond transient absorption or PTRF data presented here since the cross correlation time masks any kinetic process shorter than ~5 ps, vide supra.

As in the case of native J-625, no fluorescence is observed from J6.11 suggesting that the J intermediates have similar excited-state properties in the two photoreactions. Either no significant emission occurs or it appears outside the 650–900-nm spectral region monitored here. It is clear, however, that the ring in BR6.11 does not prevent the appearance of the J intermediate and therefore, changes in the retinal structure in the C_{11}=C_{12}—C_{13} region are not involved in the formation of J6.11, nor by analogy, of native J-625.

Fluorescence is detected from K*6.11/1 and K*6.11/2 in analogy with the observations of fluorescence from native K*-590 (16, 27). The fluorescence spectra are similar as are the intensities relative to their respective starting species. Specifically, the fluorescence quantum yields from K*6.11/1 and K*6.11/2 are comparable to that from BR*6.11. The

measured fluorescence intensity from native K*-590 is approximately two times larger than that from BR*-570 (16).

There also are important differences in the time-resolved fluorescence results from BR6.11 and native BR-570. The fluorescence spectra assignable to both K*6.11/1 and K*6.11/2 are not significantly different from each other or from that measured from BR*6.11, indicating that the emitting excited states are similar, if not the same. This contrasts with the fluorescence results from the native BR photocycle in which the spectrum from K*-590 has a blue-shifted (~15 nm) fluorescence spectrum relative to that from BR*-570 (16). The fluorescence spectrum of native K*-590 remains unchanged over the 40-ps to 80-ns time interval, although the intensity of fluorescence decreases greatly (by ~80%) (23). A more detailed examination of the fluorescence properties of this and other artificial BR pigments is needed before a molecular interpretation can be firmly established.

Comparisons of PTA and PTRF

The kinetics extracted from the PTA and PTRF data measured over the initial 5-ns period of the BR6.11 photoreaction can be readily correlated. The 12 ± 3-ps J6.11 → K6.11/1 reaction is measured independently in both PTA (Fig. 2) and PTRF (Fig. 6) data. Detecting the <5-ps appearance of J6.11 only by PTA and not by PTRF established the absence of J*6.11 fluorescence in the 650–900-nm spectral region monitored. The observation that three species with distinct absorption properties (BR6.11, K6.11/1, and K6.11/2) all have essentially the same fluorescence spectrum is unexpected. These fluorescence results suggest that the absorption transitions access different excited electronic states that subsequently reach the same emitting levels with different efficiencies. This molecular model differs from that found to describe the native BR photocycle where K-590 has a distinct fluorescence spectrum (16).

Retinal structure and photoreaction dynamics

The structural modification to the retinal backbone found in BR6.11 effectively blocks the permanent isomerization and/or rotation in the C_{11}=C_{12}—C_{13} region, but does not directly prevent C_{13}=C_{14} isomerization. The observation reported here that both J and K intermediates are part of the BR6.11 photoreaction demonstrates that substantial movement in the C_{11}=C_{12}—C_{13} region of the retinal structure is not required for either transient species to be formed. Transient distortions in the C_{11}=C_{12}—C_{13} region (e.g., twisting of the polyene backbone) remain possible in BR6.11 and, therefore, the need to have some temporary structural changes in this region are not eliminated. The previously reported observations that BR6.11 forms both an M-like intermediate and pumps protons (15) also show that neither processes requires substantial structural changes in the C_{11}=C_{12}—C_{13} region of retinal. Since isomerization at C_{13}=C_{14} remains feasible, the results reported here do not comment on the relationship between molecular motion at this point in the retinal structure and the formation of either a J or K intermediate. It has not been established whether the six-membered ring bridging the C_{11}=C_{12}—C_{13} region in BR6.11 significantly alters the chromophore-protein interactions and/or the overall protein orientation near the retinal. Consequently, no conclusions about the importance of these protein interactions in the formation of the J, K, or M intermediates and/or proton pumping can be reached yet.

The authors wish to gratefully acknowledge the technical assistance of Peter Schmidt and Dr. J. P. Jiang in recording these data and the efforts of Scott Rex, Michael Stringer, James Schmeits, and Peter Cho in the preparation of bacteriorhodopsin samples.

This work was supported by grants from the biophysics program of the National Science Foundation and the United States—Israel Binational Science Foundation.

REFERENCES

1. Ottolenghi, M., and M. Sheves. 1989. Synthetic retinals as probes for the binding site and photoreactions in rhodopsins. *J. Membr. Biol.* 112: 193–212.
2. Oesterhelt, D., C. Brauchle, N. Hampp. 1991. Bacteriorhodopsin: a biological material for information processing. *Q. Rev. Biophys.* 244: 425–478.
3. Birge, R. R. 1990. Photophysics and molecular electronic applications of the rhodopsins. *Annu. Rev. Phys. Chem.* 41:683–733.
4. Fang, J., J. Carriker, V. Balogh-Nair, and K. Nakanishi. 1983. Evidence for the Necessity of double bond (13-ene) Isomerization in the Proton Pumping of Bacteriorhodopsin. *J. Am. Chem. Soc.* 105:5162–5164.
5. Birge, R. R. 1990. Nature of the primary photochemical events in rhodopsin and bacteriorhodopsin. *Biochem. Biophys. Acta.* 1016:293–327.
6. Mathies, R., S. Lin, J. Ames, and W. Pollard. 1991. From femtoseconds to biology: mechanism of bacteriorhodopsin light driven proton pump. *Annu. Rev. Biophys. Biochem.* 20:495–518.
7. Ebrey, T. G. 1992. Light energy transduction in bacteriorhodopsin. *In* Thermodynamics of the Cell Surface Receptors. M. Jackson, editor. CRC Press, Boca Raton, FL.
8. Ottolenghi, M. 1980. The photochemistry of rhodopsin. *Adv. Photochem.* 12:97–200.
9. Harbison, G. S. Smith, J. Pirdian, J. Courtin, J. Lugtenburg, J. Henzfeld, R. Mathies, and R. Griffin. 1985. Solid state ^{13}C NMR detection of a perturbed 6-s-*trans* chromophore in bacteriorhodopsin. *Biochemistry.* 24:6955–6962.
10. Fahmy, K., F. Siebert, M. Grossjean, and P. Tuvan. 1989. Photoisomerization in bacteriorhodopsin studied by FTIR linear dichroism and photoselection experiments combined with quantum chemical theoretical analysis. *J. Mol. Str.* 214:257–288.
11. Polland, H-J., M. A. Franz, W. Zinth, W. Kaiser, E. Kölling, and D. Oesterhelt. 1984. Optical picosecond studies of bacteriorhodopsin containing a sterically fixed retinal. *Biochem. Biophys. Acta.* 767:635–639.
12. Zinth, W., J. Dobler, M. A. Franz, and W. Kaiser. 1988. The primary steps of photosynthesis in bacteriorhodopsin. *In* Spectroscopy of Biological Molecules - New Advances. E. Schmid, F. W. Schreilder, and F. Sieberts, editors. John Wiley & Sons, New York. 269–274.
13. Noguchi, T., S. Kolaczkowski, W. Gärtner, and G. H. Atkinson. 1990. Resonance Raman spectra of 13-demethylretinal bacteriorhodopsin and of a picosecond bathochromic photocycle intermediate. *J. Phys. Chem.* 94 12: 4920–4926.
14. Brack, T. L., W. Gärtner, and G. H. Atkinson. 1992. Picosecond time-resolved fluorescence spectroscopy of 13-demethylretinal bacteriorhodopsin. *Chem. Phys. Lett.* 190(3, 4):298–304.
15. Albreck, A., N. Freidman, M. Sheves, and Ottolenghi. 1986. Role of retinal isomerization and rotations in the photolysis of bacteriorhodopsin. *J. Am. Chem. Soc.* 108:614–618.

16. Atkinson, G. H., T. L. Brack, D. Blanchard, and G. Rumbles. 1991. Picosecond time-resolved fluorescence spectroscopy of K-590 in the bacteriorhodopsin photocycle. *Biophys. J.* 55:263–274.

17. Blanchard, D., D. A. Gilmore, T. L. Brack, H. Lemaire, and G. H. Atkinson. 1991. Picosecond time-resolved absorption and fluorescence spectroscopy in the bacteriorhodopsin photocycle. *Chem. Phys.* 154: 155–170.

18. Clemens, J. M., J. Najbar, I. Bronstein-Bronte, and R. M. Hochstrasser. 1983. Dual picosecond dye lasers synchronously pumped by a mode-locked cw YAG laser. *Opt. Comm.* 47:271–277.

19. Shichida, Y., S. Matuoka, Y. Hidaka, and T. Yoshizawa. 1984. Absorption spectra of intermediates of bacteriorhodopsin measured by laser photolysis at room temperature. *Biochem. Biophys. Res. Commun.* 273: 240–246.

20. Polland, H-J., M. A. Franz, W. Zinth, W. Kaiser, E. Kolling, and D. Oesterhelt. 1986. Early events in the photocycle of bacteriorhodopsin. *Biophys. J.* 49:651–662.

21. Lewis, A., J. P. Spoonhower, and G. S. Perreault. 1976. Observation of light emission from a rhodopsin. *Nature (Lond.).* 260:675–678.

22. Milder, S. J., and D. S. Kliger. 1988. A time resolved spectral study of the K and KL intermediates of bacteriorhodopsin. *Biophys. J.* 53: 465–468.

23. Delaney, J. K., T. L. Brack, and G. H. Atkinson. 1993. Time-resolved absorption and fluorescence from the bacteriorhodopsin photocycle in the nanosecond time regime. *Biophys. J.* (In press).

24. Brack, T. L., and G. H. Atkinson. 1991. Vibrationally excited retinal in the bacteriorhodopsin photocycle: picosecond time-resolved anti-Stokes resonance Raman scattering. *J. Phys. Chem.* 95:2351–2356.

25. Doig, S. J., P. J. Reid, and R. A. Mathies. 1991. Picosecond time-resolved resonance Raman spectroscopy of bacteriorhodopsin's J, K, and KL intermediates. *J. Phys. Chem.* 95:6372–6297.

26. Balashov, S., N. Karneyeva, F. Litvin, and T. Ebrey. 1991. Bathoproducts and conformers of all-*trans* and 13-*cis* BR at 90K. *Photochem. Photobiol.* 54:949–953.

27. Atkinson, G. H., and T. L. Brack. 1991. Fluorescence from the primary products of the bacteriorhodopsin photocycle: picosecond time-resolved fluorescence spectroscopy. *J. Lumin.* 48–49:410–414.